

Molecular Sieving Using Single Wall Carbon Nanotubes

Gaurav Arora and Stanley I. Sandler*

Center for Molecular and Engineering Thermodynamics, Department of Chemical Engineering, University of Delaware, Newark, Delaware 19716

Received September 18, 2006; Revised Manuscript Received December 10, 2006

ABSTRACT

By using molecular dynamics and grand canonical Monte Carlo simulations, we find that a nanotube with a constriction results in high transport resistance to nitrogen while allowing oxygen to pass at a much higher rate even though these gases have very similar sizes and energetics. This provides an understanding of the reported high permeation rates of oxygen relative to nitrogen in nanoporous carbon membranes and a basis for designing nanotubes with constrictions using available technologies for membrane-based separations.

Possible alternatives to the energy intensive cryogenic distillation of air are separations based on polymeric, zeolitic, and carbon molecular sieves membranes. The effectiveness of membrane-based separations has been shown to be bounded by a tradeoff between selectivity and permeability, with higher permeability resulting in lower selectivity, as was initially shown for polymeric membranes.¹ Carbon molecular sieves and zeolitic membranes have been shown to lie above the polymer membrane upper-bound region, and there is continuing interest in identifying new molecular sieving materials with even better selectivity and permeability.

Carbon nanotubes offer the possibility of improving the selectivity/permeability bound as they exhibit significantly higher fluxes than other membrane materials, as was first shown by Skoulidas et al. using molecular dynamics simulations.² The primary reasons being the axial smoothness of the interaction of the molecules with the carbon nanotube walls resulting in large transport diffusion coefficients. For the same reasons, 4 to 5 orders of magnitude faster fluid velocities than conventional fluid flow have been observed in the pressure-driven flow of liquids through aligned multiwalled carbon nanotubes.³ In agreement with previous molecular simulations, recent gas flow measurements of N₂, O₂, and other gases through carbon nanotube-based membranes showed that these membranes have permeabilities more than an order of magnitude larger than the current commercial polycarbonate membranes.⁴

It has been suggested that single walled carbon nanotubes (SWCN) could therefore be used to synthesize membranes with both high selectivity and high fluxes, overcoming the limitation in current membranes. However, although nanotube membranes have high flow rates, their selectivity to

the gases followed the inverse-square-root scaling to molecular mass so that no significant selectivity was observed.⁴ The purpose of this work is to demonstrate that it is possible with current technology to tailor carbon nanotubes that also exhibit molecular sieving and therefore that it is possible to design membranes with both high selectivity and mass transport.

It has appeared that molecular sieving, although desirable, is difficult to produce using carbon nanotubes due to the discrete dependence of nanotube diameter on their chiral indices. A further complication in the separation of air is the very similar kinetic diameters of nitrogen (3.64 Å) and oxygen (3.46 Å).⁵ Here we demonstrate using atomistic simulations of N₂ and O₂ in single wall carbon nanotubes with constrictions (that we denote as SWCN-C) that even the very small difference in the molecular sizes of N₂ and O₂ is sufficient to provide large sieving resistance to nitrogen in specially tailored carbon nanotubes. These simulations suggest a method of designing carbon nanotube-based membranes for highly effective air separation and a model that can be used for designing membranes for other separations.

These simulations also provide an understanding of the mechanism for the separation of similarly sized gas molecules using nanoporous carbon materials. In particular, carbon molecular sieve (CMS) membranes have shown a wide range of O₂/N₂ selectivities depending on the polymer precursor, the pyrolysis conditions, and other factors.⁶ Recently Foley and co-workers synthesized nanoporous CMS membranes by the pyrolysis of ultrasonically deposited polyfurfuryl alcohol that showed an ideal selectivity of O₂ over N₂ ranging from 3 to 30 depending on the membrane synthesis conditions.⁷ These amorphous nanoporous membranes undoubtedly contained pores with bends and other

* Corresponding author. sandler@udel.edu. Telephone: (302)-831-2945. Fax: (302)-831-3226.

constrictions so that the SWCN-C considered here also provides an explanation for their experimental data.

Separations using CMS membranes are due to the combination of an entropic effect arising from the difference in size of adsorbate molecules and an enthalpic effect that primarily depends on the adsorbate–adsorbent interactions. As N_2 and O_2 have very similar molecular sizes and interaction energies, the reason for this large difference in pure component permeabilities has not been clear, and molecular level studies using transition state theory have appeared that support both entropic⁸ and enthalpic arguments.^{9,10} Molecular simulations using model representations of CMS membranes that have ranged from simple graphitic slit pores¹¹ and more complicated structures such as C_{168} schwarzite¹² have resulted in only moderate O_2/N_2 selectivities, not the high ideal selectivity found by Foley et al.⁷ Also, as described elsewhere,¹² using more accurate force fields obtained from quantum mechanics¹³ resulted in only somewhat higher O_2/N_2 selectivity than using the empirical potentials¹⁴ and did not explain the high selectivities observed in experiment. The conclusion from these simulations is that the energetic contribution to the selectivity alone could not explain the large differences in the permeation rates.

The use of CMS for pressure swing adsorption is based on the accurate control of the sizes of pore channels and pore mouths, an entropic effect. It is known that CMS adsorbents with mean pore sizes ranging from 4 to 5 Å can offer significantly more resistance to the adsorption of nitrogen than to oxygen, although kinetic diameters differ by only 0.18 Å.¹⁵ Using atomistic simulations to model molecular sieving through CMS remains a challenge due to their amorphous nature so that it is not possible to determine the exact carbon coordinates. This is further complicated by the sensitive dependence of the separation properties on the membrane synthesis conditions. Small changes in the mean pore size and the pore size distribution result in considerable changes in the selectivity.

The introduction of a pair of heptagonal and pentagonal carbon rings in a carbon nanotube results in a constriction that can be viewed as two nanotubes of different diameters joined together by a truncated conical honeycomb lattice.¹⁶ Geometrically such a junction is aligned or bent at various angles depending on the chirality of nanotubes, i.e., armchair, zigzag, or chiral, and the relative location of the pentagonal and hexagonal carbon rings. Two special cases are a straight junction between nanotubes of the same helicity¹⁷ and a junction with a bend angle of approximately 36° formed between zigzag and armchair nanotubes, with pentagonal and hexagonal carbon rings located at the diametrically opposite ends of the nanotube.¹⁸ It has been shown that such topological defects in the form of nonhexagonal carbon rings can arise during the growth process,¹⁹ can be induced using electron irradiation²⁰ or by applying a tensile load.²¹ Also, the presence of adatoms and tension has been shown to result in a constriction by the controlled formation of short segments of different helicity in the parent nanotube.²²

We have used the algorithm of Melchor and Dobado²³ that generates the coordinates of the carbon atoms in joining two



Figure 1. Nanotube with constriction constructed by joining (17,0) and (9,0) nanotubes with diameters 13.31 and 7.05 Å, respectively

nanotubes with any arbitrary (n,m) indices to construct a single walled nanotube of total length 108.7 Å with a constriction (SWCN-C) by joining (17,0) and (9,0) nanotubes. These nanotubes have diameters (carbon center-to-center distances) of 13.31 and 7.05 Å, respectively. The SWCN-C generated is shown in Figure 1 and will be referred to as 17000900-SWCN-C. Grand canonical Monte Carlo and equilibrium molecular dynamics simulations were used to study the adsorption and diffusion of pure N_2 and O_2 in this nanotube. GCMC simulations consisted of an equilibration period of 10^7 standard trial moves followed by a sampling period of 2×10^7 trial moves.²⁴ In EMD simulations, the system was allowed to equilibrate for 0.5 ns, followed by a sampling period of 100 ns. A cut off of 13 Å was used to truncate adsorbate–adsorbate and adsorbate–adsorbent interactions. The force field describing molecular interactions and other simulation details have been described elsewhere.^{25–27}

First, to gauge the sieving capabilities of the constriction, the ends were sealed with planar graphite sheets and an initial configuration of adsorbed molecules was generated by inserting 20 molecules of either nitrogen or oxygen into one side of the constriction using GCMC simulation. Then EMD simulations were performed and the numbers of molecules on each side of a plane dividing the nanotube into two halves were recorded as a function of time. The results are shown in Figure 2 where each step denotes a passing of molecule across the plane dividing the constriction. Passing of N_2 is a rare event, as seen in Figure 2a, with an average of 3.4 passings per ns (3.4/ns) of simulation compared to oxygen molecules that pass at the much higher rate of 145.4/ns, as shown in Figure 2b. Also, starting with 20 molecules of a pure gas on one side of the constriction, the first instance when there are an equal number of molecules on each side of the nanotube is 0.650 ns for O_2 and 15.7 ns for N_2 .

We next performed EMD simulations for an open-ended 17000900 SWCN-C with periodic boundary conditions along the axis of the nanotube, which can be thought of as an infinitely long nanotube formed by periodic joinings of (17,0) and (9,0) nanotubes. The starting configuration of 40 adsorbate molecules (3.7 molecules/nm) in the SWCN-C was generated from grand canonical Monte Carlo simulations. This adsorbate loading corresponds to bulk pressures of 21.2 and 12.6 bar for N_2 and O_2 , respectively (see Figure 4). As shown in Figure 3, using the EMD simulations the mean-square displacement along the axis of the nanotube was found to be linear for O_2 in the limit of long time and corresponds to a self-diffusion coefficient D_s of $7.3 (\pm 0.5) \times 10^{-5} \text{ cm}^2/\text{s}$. However, nitrogen is essentially confined to the region between constrictions, resulting in an almost asymptotic behavior of the mean-square displacement at long times so

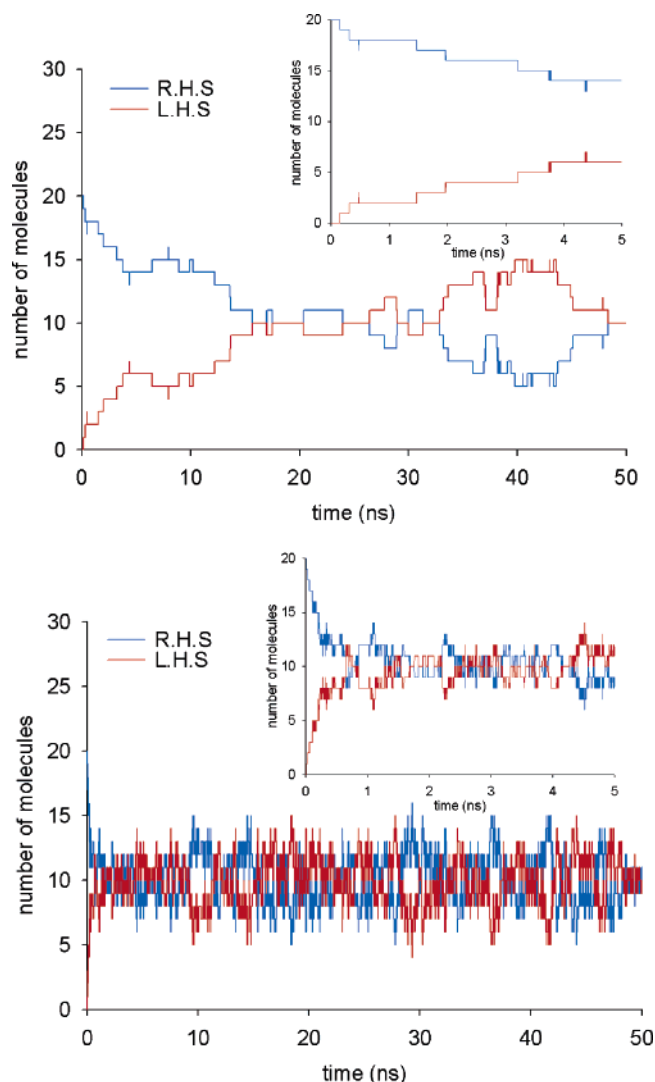


Figure 2. Number of (a) N_2 and (b) O_2 molecules on either side of the constriction in a 17000900-SWCN-C as a function of time. Both ends of the SWCN-C were sealed using a planar graphite sheet, and the starting configuration had 20 adsorbate molecules on one side of the constriction. The inset shows the results on a larger scale.

that a diffusion coefficient cannot be computed. The transport diffusion coefficient, D_t , of oxygen was calculated as $9.2 (\pm 1.9) \times 10^{-4} \text{ cm}^2/\text{s}$. At the same operating pressure of 12.6 bar, the D_s and D_t of O_2 in a straight (17,0) nanotube were found to be $2.3 (\pm 0.2) \times 10^{-3} \text{ cm}^2/\text{s}$ and $1.1 (\pm 0.1) \times 10^{-1} \text{ cm}^2/\text{s}$, respectively. We note that, upon introduction of the constriction in a straight (17,0) nanotube, there is a significant drop in the D_s and D_t , as would be expected. However, the observed D_t of O_2 in SWCN-C is still orders of magnitude higher than other nanoporous materials that separate N_2 and O_2 by exploiting the difference in their diffusion rates. For example, close to room temperature, the typical transport diffusivities of O_2 in zeolite 4A are $\sim 10^{-8} \text{ cm}^2/\text{s}$ ²⁸ and for CMS transport diffusivities ranging from $\sim 10^{-7}$ – $10^{-8} \text{ cm}^2/\text{s}$ has been measured depending on the polymer precursor used and the synthesis conditions.^{29,30}

This preferential selectivity of allowing oxygen over nitrogen to pass through the constriction despite their similar

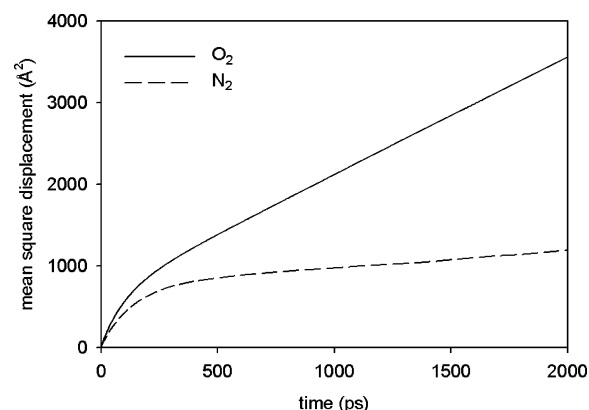


Figure 3. Mean square displacement of pure N_2 and O_2 in the 17000900-SWCN-C as a function of time

molecular sizes and energetics can be seen in the media files of the simulation in the Supporting Information. One point to be noted in these simulation files is that the oxygen molecules can rotate within the constriction, while a nitrogen molecule cannot, so that nitrogen has to be properly oriented to enter the constriction. Second, there is an important rotational entropy contribution to the selectivity, as within the constriction oxygen retains but nitrogen loses its rotational degrees of freedom (DOF). That is, a nitrogen molecule must be aligned along the axis of the constriction to enter and pass through it, while oxygen can enter the constriction in any orientation and rotate within it. A statistical mechanics analysis for the similar case of N_2 and O_2 diffusion in a CMS of disrupted graphite slit pores by Singh and Koros⁸ using transition state theory (TST) also suggests a significant entropic contribution to selectivity that is supported by the simulation results and media files of this work.

Our simulations predict that, as the result of an appropriately sized constriction, it is possible to selectively transport oxygen but not nitrogen through carbon nanotubes despite their very similar molecular sizes. An aligned carbon nanotube membrane synthesized using nanotubes with the appropriate constriction can therefore offer significant improvement over current limits of both selectivity and mass transport. A different type of size effect was also observed previously for the straight (17,0) nanotube at high loadings wherein the slightly smaller O_2 was found to form two internal adsorption layers, while N_2 adsorbed only in a single annular layer close to the carbon wall.²⁶ However, this did not explain the large differences in mass transport rates that had been found in experiment.

From energetic arguments, all space in the constricted nanotube is available for adsorption by N_2 and O_2 and has been sampled by both gases in GCMC simulations, as shown in the insets in Figure 4. We also see that the equilibrium adsorption behavior of pure O_2 and pure N_2 are very similar, with only moderate differences at high pressures. However, from the results of EMD simulations, we can see that equilibrium will be achieved much more slowly for N_2 than for O_2 . The similarity in equilibrium adsorption combined with the significant difference in permeabilities suggests that a separation based on adsorption equilibrium in carbon

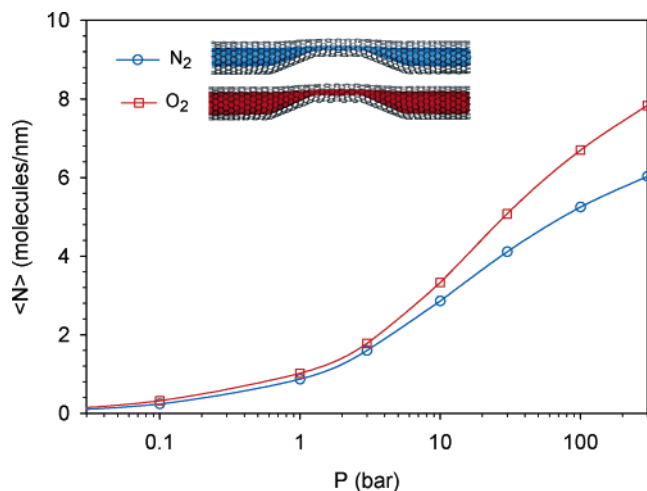


Figure 4. Adsorption isotherms of pure N₂ (blue) and O₂ (red) in the 17000900-SWCN-C at 298 K. The inset shows the equilibrium configuration space sampled by N₂ and O₂ inside the nanotube at 298 K and 300 bar obtained by plotting 100 equilibrium configurations.

nanotubes will not be useful, however, a separation based on the kinetics of adsorption,¹⁵ which can exploit the high resistance offered by the constriction to nitrogen compared to that for oxygen, can result in high selectivities.

As demonstrated by Seaton et al.³¹ using pore network theory, the transport of a chemical species is dominated by the smallest pore size or the constriction offering the maximum resistance. The results in this work demonstrate that this entropic effect can explain the large O₂/N₂ selectivities experimentally observed in real carbon molecular sieve membranes. The approximate pore size for 17000900-SWCN-C constriction, calculated using $d_{\text{SWCN}} - \sigma_{\text{CC}}$, where d_{SWCN} is the nanotube diameter and $\sigma_{\text{CC}} = 3.4 \text{ \AA}$ ¹⁴ is the carbon collision diameter, is 3.65 Å. This is in agreement with the current consensus that a pore size of about 4 Å or less is required for the separation of N₂ and O₂ using CMS.^{8,10,15}

To explore the utility of nanotubes with constrictions for equilibrium-based separations, we computed the equilibrium adsorption capacity for oxygen and nitrogen obtained using GCMC simulations of carbon nanotubes with a collection of different internal diameters at 10 bar and 298 K, and the results are shown in Figure 5. It is interesting that the dependence of adsorption density or loading is smooth and does not show any irregularities with changing nanotube chirality. This suggests that there is a great deal of flexibility in designing a nanotube-based membrane despite the fact that the diameter of nanotubes, and hence the constrictions, are determined by the (n,m) indices of the nanotubes and therefore vary in a discrete manner.

The nanotubes with diameter smaller than that of the (9,0) nanotube, that is the (7,2), (8,1), (5,5), and (6,4) nanotubes, show large differences in adsorbate loading of N₂ and O₂ (Figure 5). However, these results were obtained from GCMC simulations that use random insertion and deletion moves within the nanotube to obtain thermodynamic equilibrium between the adsorbate and bulk phase and does not

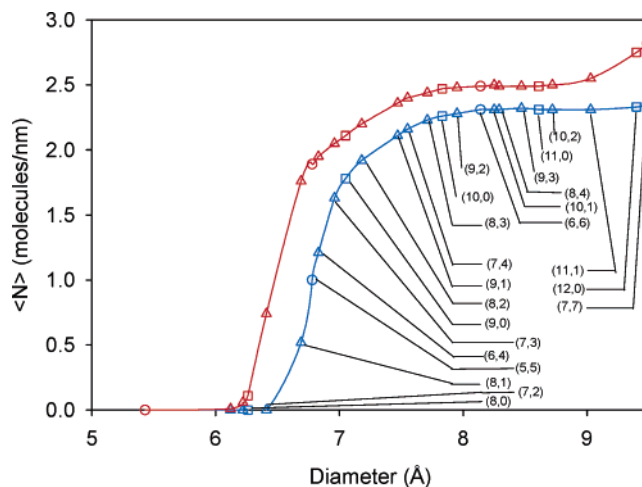


Figure 5. Adsorbed loading of N₂ (blue) and O₂ (red) in a collection of single wall carbon nanotubes of varying diameter and different chiralities at 298 K and 10 bar. Results for armchair ($n = m$), zigzag ($m = 0$) and chiral ($n \neq m$) nanotubes are shown by circles, squares, and triangles, respectively. The lines are there to guide the eye.

take into account the entrance effect of the narrow pore size constrictions. Therefore, to understand the possible sieving capabilities of these smaller constrictions, we also performed the EMD simulations on 10100702-SWCN-C and 10100505-SWCN-C with constriction pore sizes of 3.01 and 3.38 Å, respectively. There we found that due to the small pore sizes of these constrictions, it is very difficult for either O₂ or N₂ to enter the constriction. This resulted in zero passing of N₂ and O₂ in the 10100702-SWCN-C, zero passing for N₂, and passing of O₂ only at a rate of 10.8 /ns in the 10100505-SWCN-C. This was not unexpected because these constrictions have a smaller diameter than suggested in the literature for possible N₂/O₂ separation using a CMS. From these results and Figure 5, although not definitive as they are based on equilibrium not transport simulations, we expect that (8,1), (5,5), (6,4), and (9,0) nanotubes to result in molecular sieving of oxygen in preference to nitrogen, with the (9,0) nanotube used for the constriction here, resulting in the largest effect.

It should be pointed out that the smoothness of the interaction between the adsorbate molecules and the carbon nanotubes walls results in the gas high transport rates, but plays little role in the transport selectivity. The dominant effect is sieving due to the size difference of the molecules. However, as the transport rate is considerably decreased when the nanotube diameter is sufficiently small that molecular sieving occurs, a larger diameter nanotube with a localized molecular sieving constriction should result in higher transport rates than if the whole nanotube had the molecular sieving diameter.

To summarize, despite the similar sizes of N₂ and O₂ and the discrete variation of nanotube diameters with the (n,m) indices of SWCNs, it is possible to identify a technically possible pore size constriction that leads to a high sieving resistance for N₂ but not for O₂, resulting in a SWCN-C membrane with high selectivity for air separation. Similarly, for other industrial separation processes in which there are small differences in the sizes of the mixture components,

the identification of a correct nanotube and constriction size should be possible for high permeability and selectivity, which then could be fabricated by the processes mentioned earlier. The high selectivities resulting from the ability to tailor their structures combined with the high permeation rates found in carbon nanotubes make them very attractive for membrane-based separation processes, as they can offer significant improvements over the current separation technologies.

Acknowledgment. This research was supported by grant number CTS-0083709 from the National Science Foundation, and contract DE-FG02-85ER13436 from the Basic Energy Sciences Division of the U.S. Department of Energy.

Supporting Information Available: Nitrogen 1700-0900 SWCN with constriction; oxygen 1700-0900 SWCN with constriction (MPEG files). Animation from nitrogen and oxygen transport through 17000900-SWCN-C at 298 K. This material is available free of charge via the Internet at <http://pubs.acs.org>.

References

- (1) Robeson, L. M. *J. Membr. Sci.* **1991**, *62*, 165–185.
- (2) Skoulidas, A. I.; Ackerman, D. M.; Johnson, J. K.; Sholl, D. S. *Phys. Rev. Lett.* **2002**, *89*, 185901.
- (3) Majumder, M.; Chopra, N.; Andrews, R.; Hinds, B. J. *Nature* **2005**, *438*, 44–44.
- (4) Holt, J. K.; Park, H. G.; Wang, Y.; Stadermann, M.; Artyukhin, A. B.; Grigoropoulos, C. P.; Noy, A.; Bakajin, O. *Science* **2006**, *312*, 1034–1037.
- (5) Verma, S. K. *Carbon* **1991**, *29*, 793–803.
- (6) Saufi, S. M.; Ismail, A. F. *Carbon* **2004**, *42*, 241–259.
- (7) Shiflett, M. B.; Foley, H. C. *Science* **1999**, *285*, 1902–1905.
- (8) Singh, A.; Koros, W. J. *Ind. Eng. Chem. Res.* **1996**, *35*, 1231–1234.
- (9) Rallabandi, P. S.; Ford, D. M. *AIChE J.* **2000**, *46*, 99–109.
- (10) Acharya, M.; Foley, H. C. *AIChE J.* **2000**, *46*, 911–922.
- (11) Travis, K. P.; Gubbins, K. E. *Mol. Simul.* **2001**, *27*, 405–439.
- (12) Arora, G.; Sandler, S. I. *Langmuir* **2006**, *22*, 4620–4628.
- (13) Klauda, J. B.; Jiang, J.; Sandler, S. I. *J. Phys. Chem. B* **2004**, *108*, 9842–9851.
- (14) Bojan, M. J.; Steele, W. A. *Langmuir* **1987**, *3*, 1123–1127.
- (15) Gaffney, T. R. *Curr. Op. Solid State Mater. Sci.* **1996**, *1*, 69–75.
- (16) Saito, R.; Dresselhaus, G.; Dresselhaus, M. S. *Phys. Rev. B* **1996**, *53*, 2044–2050.
- (17) Meunier, V.; Nardelli, M. B.; Roland, C.; Bernholc, J. *Phys. Rev. B* **2001**, *64*, 195419.
- (18) Dunlap, B. I. *Phys. Rev. B* **1994**, *49*, 5643–5650.
- (19) Iijima, S.; Ichihashi, T.; Ando, Y. *Nature* **1992**, *356*, 776–778.
- (20) Ajayan, P. M.; Ravikumar, V.; Charlier, J. C. *Phys. Rev. Lett.* **1998**, *81*, 1437–1440.
- (21) Yakobson, B. I. *Appl. Phys. Lett.* **1998**, *72*, 918–920.
- (22) Orlikowski, D.; Nardelli, M. B.; Bernholc, J.; Roland, C. *Phys. Rev. Lett.* **1999**, *83*, 4132–4135.
- (23) Melchor, S.; Dobado, J. A. *J. Chem. Inf. Comput. Sci.* **2004**, *44*, 1639–1646.
- (24) Allen, M. P.; Tildesley, D. J. *Computer Simulation of Liquids*; Oxford University Press: Oxford, 1987.
- (25) Arora, G.; Wagner, N. J.; Sandler, S. I. *Langmuir* **2004**, *20*, 6268–6277.
- (26) Arora, G.; Sandler, S. I. *J. Chem. Phys.* **2005**, *123*, 044705.
- (27) Arora, G.; Sandler, S. I. *J. Chem. Phys.* **2006**, *124*, 084702.
- (28) Karger, J.; Ruthven, D. M. *Diffusion in Zeolites and Other Microporous Solids*; John Wiley: New York, 1992.
- (29) Strano, M. S.; Foley, H. C. *Carbon* **2002**, *40*, 1029–1041.
- (30) Kim, Y. K.; Park, H. B.; Lee, Y. M. *J. Membr. Sci.* **2004**, *243*, 9–17.
- (31) Seaton, N. A.; Friedman, S. P.; MacElroy, J. M. D.; Murphy, B. J. *Langmuir* **1997**, *13*, 1199–1204.

NL062201S